



# **Petrography and Geochemistry of the Harzburgite Xenoliths of Lake Guinnadji and Ngao Djalsoka Volcano from the Dibi Area (Adamawa Plateau - Cameroon)**

**H. Adama<sup>a</sup>, O. F. Nkouandou<sup>a</sup>, J. M. Bardintzeff<sup>b\*</sup>, M. Y. Mbainassem<sup>a</sup>,  
N. M'Non-Allah<sup>a</sup>, L. C. Okomo Atouba<sup>c</sup> and Z. N. Njankouo Ndassa<sup>a</sup>**

<sup>a</sup> Department of Earth Sciences, Faculty of Sciences, University of Ngaoundéré, P.O.Box 454, Ngaoundéré, Cameroon.

<sup>b</sup> Univ Paris-Saclay, Sciences de la Terre, Volcanologie-Planétologie, UMR CNRS 8148 GEOPS, Bât. 504, F-91405 Orsay, France.

<sup>c</sup> Higher Teacher Training College of Bertoua, University of Ngaoundéré, P.O.Box 652, Bertoua, Cameroon.

## **Authors' contributions**

*This work was carried out in collaboration among all authors. All authors read and approved the final manuscript.*

## **Article Information**

DOI: 10.9734/JGEESI/2021/v25i1030324

### Editor(s):

(1) Dr. Wen-Cheng Liu, National United University, Taiwan.

### Reviewers:

(1) R. Dhana Raju, India.

(2) Laishram Sarjesh Singh, India.

Complete Peer review History, details of the editor(s), Reviewers and additional Reviewers are available here:  
<https://www.sdiarticle5.com/review-history/81483>

**Original Research Article**

**Received 20 October 2021**

**Accepted 22 December 2021**

**Published 23 December 2021**

## **ABSTRACT**

Petrographic and geochemical studies have been carried out on the peridotite xenoliths included in the pyroclastite deposits from the Lake Guinnadji and Ngao Djalsoka volcano close to the Dibi locality in the Adamawa plateau, central Cameroon. The peridotite xenoliths exhibit protogranular and porphyroclastic textures, and are composed of olivine, orthopyroxene and minor amount of clinopyroxene, amphibole (?) and spinel, typical of harzburgite type. ICP-MS and ICP-OES analyses of representative samples show that they are in the range of those of the primitive mantle origin (42.4-45.0 wt.% MgO, 65.7-79.0 wt.% normative olivine). Decreasing SiO<sub>2</sub>, TiO<sub>2</sub>, Al<sub>2</sub>O<sub>3</sub> and CaO contents vs increasing MgO trends evidence depletion from more fertile mantle by extraction

\*Corresponding author: E-mail: [jacques-marie.bardintzeff@universite-paris-saclay.fr](mailto:jacques-marie.bardintzeff@universite-paris-saclay.fr);

of basaltic melts, leaving a refractory residue of harzburgite composition. High contents of REE and incompatible elements point out secondary enrichment processes which have affected the peridotite xenoliths. For this, metasomatism caused by silicate fluids is invoked. In that way, peridotite of Dibi area witness of the nature and the evolution of lithospheric mantle under the Adamawa plateau.

**Keywords:** Mantle xenoliths; harzburgite; melt extraction; metasomatism; Adamawa plateau; Cameroon.

## 1. INTRODUCTION

The basement of African continent is composed of the Archean cratons and Pan African mobile belts (Fig. 1A). The Cameroon volcanic line and Adamawa plateau (Fig. 1B) are among the main volcanic structures located within the Pan African belt. The studied area (Fig. 1C) belongs to the central Adamawa plateau that is an asymmetrical horst of mean altitude of 1100 m with 1 km difference in height vis-à-vis to its vicinity. The horst shape structure of Adamawa took place during the Tertiary times after its uplift due to the reworking of Pan African faults [1] which delimit its northern and southern borders that form cliffs in the landscape. Geophysical studies carried out on the Adamawa plateau have shown that Pan African faults have cut the crust down to the mantle [2,3] and thus have served as natural passage for the magma to reach the surface [1], probably after the mantle melting through adiabatic decompression process [4]. Adamawa uprising could have break up the crust-mantle equilibrium system [5], leading to the evolution of the subcontinental mantle with the modification of

its nature, structure and composition [6,7,5]. This evolution is ascertained by previous studies on mantle materials brought to the surface by Mio-Pliocene basaltic lavas flows, which have shown that the nature of subcontinental mantle beneath the Adamawa plateau seems rather complex [8,6,7] due to it heterogeneous composition, not yet cleared up. Recent petrological studies [7,5] suggest that spinel lherzolites from Youkou (south-east of Ngaoundéré) and from the area north of Ngaoundéré have been affected by late metasomatic enrichment induced by hydrous silicate melts and that they must have experienced refertilization processes driven by the infiltration of carbonatite or carbonated silicate melts.

The present work concerns the recently collected peridotite xenoliths from the Lake Guinnadji and Ngao Djalsoka volcano close to the Dibi locality (35 km south of Ngaoundéré) and focuses on their petrographic and geochemical features in order to allow new insights in the nature of Adamawa mantle and its evolution processes.

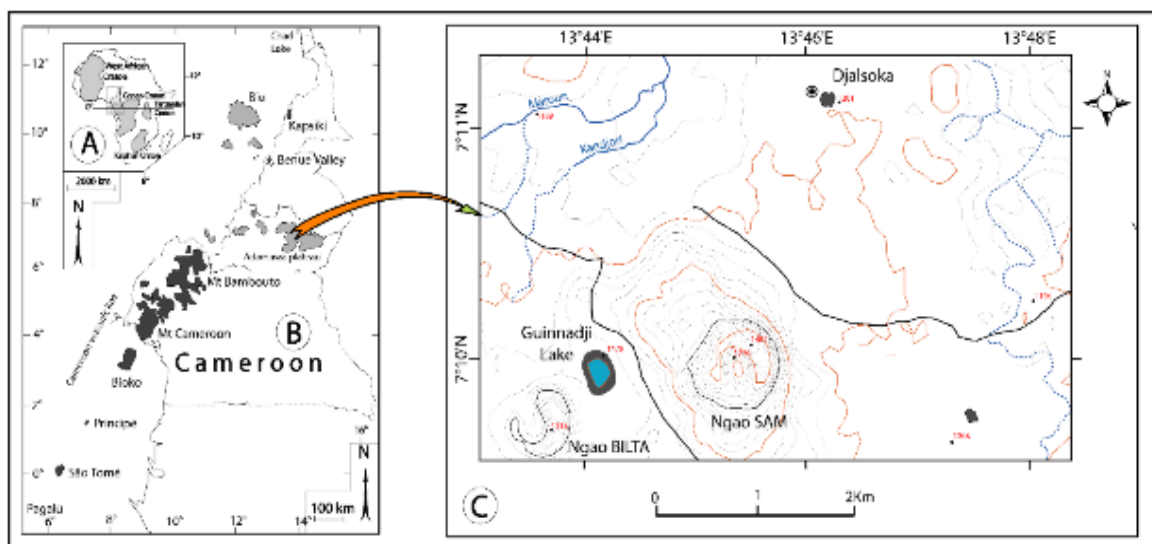


**Fig. 1. A: Main African cratons, B: Cameroon volcanic line and Adamawa plateau volcanic area (modified after Kampunzu and Popoff, [9]; Déruelle et al., [10]), C: Location of studied area of the Guinnadji Lake and Djalsoka volcano**

## 2. GEOLOGICAL SETTING

Lake Guinnadji and Ngao Djalsoka are the volcanic structures close to the Dibi locality, which belong to the Adamawa plateau that is a horst of Pan African basement including 630–620 Ma pre- to syn-D1, 580–600 Ma syn-D2 and 550 Ma post-orogenic granitoids [11,12,13]. The basement is also composed of pyroxene-and amphibole-bearing gneiss located in the south of Meiganga, showing the geochemical characteristics of Archean TTG (tonalite - trondhjemite - granodiorite), dated of Late Archean (2.6 Ga) to Paleoproterozoic (1.7 Ga) ages by  $^{207}\text{Pb}/^{206}\text{Pb}$  single-zircon evaporation method [14]. The recent volcanic episode of Adamawa plateau, dated at  $0.91 \pm 0.06$  Ma, yielded maars and scoria cones with associated basaltic lava flows [15], mainly around Ngaoundéré. At the center of Ngaoundéré area, Adamawa basement is covered by basaltic and felsic volcanic lavas of Mio-Pliocene age of 7 to 11 Ma [16,15,17]. In the Dibi locality, hillocks of dome shape are composed exclusively of pyroclastite projections which freshness should witness of the most recent volcanic ages. The studied peridotite xenoliths have been sampled in pyroclastite projections of Dibi. Petrography and mineralogical studies carried out on the Dibi lherzolite peridotites [18] sampled from the mantle by pyroclastite projections on their way to the surface have shown that the Moho discontinuity is located at a depth of 20 km, after the whole Adamawa uplift at Tertiary times.

## 3. ANALYTICAL METHODS

Studied peridotites recently discovered in the pyroclastite projections of Dibi locality have undergone petrographic studies using 10 thin sections prepared at the laboratory GEOPS, University Paris-Saclay, France. Modal proportions of different mineral phases (olivine, orthopyroxene, clinopyroxene, spinel, plus amphibole (?)) of studied peridotite xenoliths selected for this work have been estimated under a polarizing microscope. Major element analyses have been carried out by ICP-OES (Inductively Coupled Plasma - Optical Emission Spectrometry) and trace element analyses by ICP-MS (Inductively Coupled Plasma - Mass Spectrometry) at the Acme Labs of Vancouver, Canada. For the preparation of samples, about 300 mg of powder have been treated with  $\text{LiBO}_2/\text{Li}_2\text{B}_4\text{O}$  flux and dissolved in  $\text{HNO}_3$ . Crucibles are fused in a furnace. The cooled bead is dissolved in ACS grade nitric acid. Loss

on ignition (LOI) was determined by igniting a sample split then measuring the weight loss. For ICP-MS analyses of trace and REE elements, a 0.25 g split is heated in  $\text{HNO}_3\text{-HClO-HF}$  to fuming and taken to dryness. The residue is dissolved in HCl.

## 4. RESULTS

### 4.1 Field Work

Studied samples are collected from the pyroclastite deposits around Lake Guinnadji and Ngao Djalsoka volcano (Fig. 2A) close to the Dibi locality (Table 1): both belong to the same volcanic episode aged of  $0.91 \pm 0.06$  Ma [19]. Ngao Djalsoka belongs to a ENE trend of volcanic cones (Fig. 1C). Of many volcanoes in the area, Ngao Djalsoka is composed of various types of pyroclastite projections including welded tuffs (including blocks of 5-20 cm in size), bombs (10-30 cm in size) and rare blocks 30-60 cm in size, with some showing porous structure, lapilli, volcanic ashes, and in addition some roped lava flows (Fig. 2B, C, D). Pyroclastite projections around Lake Guinnadji and Ngao Djalsoka volcano have the same mineral composition: yellowish or bluish olivine crystals, blackish pyroxene crystals and tiny sparkling plagioclase microlites.

Studied peridotite xenoliths have been found in such basaltic blocs (Fig. 2). They exhibit yellowish (Fig. 2B) or blackish colour (Fig. 2C). They are sub-rounded or sub-angular in shape and show sharp contacts with basaltic host lava (Fig. 2D). The main distinguished minerals of peridotite xenoliths are blue yellowish olivine crystals (60 to 70 volume %) and undistinguished blackish ones (pyroxene, amphibole or spinel?). Whitish crumbly fragments (5 to 7 cm) of crustal origin are packed up in the matrix. The contact between crustal enclave and basaltic host lava show a thin brown corona.

### 4.2 Petrography

Under the plane polarized light (Fig. 3), Lake Guinnadji and Djalsoka volcano xenoliths exhibit protogranular (Fig. 3A and B) or porphyroclastic texture (Fig. 3C and D), following the nomenclature of Mercier and Nicolas (1975). All selected samples are mainly composed of olivine, orthopyroxene, clinopyroxene, amphibole (?) and  $\pm$  spinel. Large crystals (olivine, orthopyroxene, clinopyroxene) are outlined by dots in the borders.

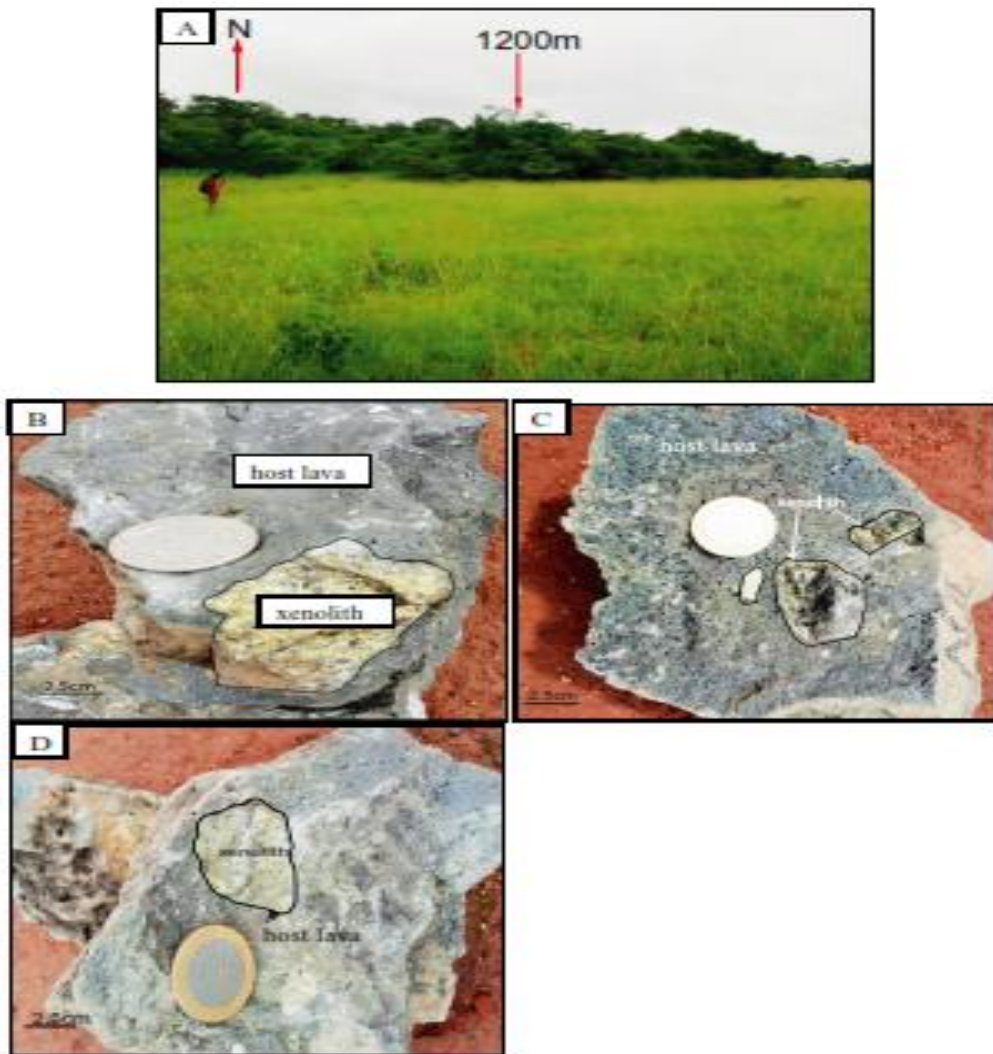
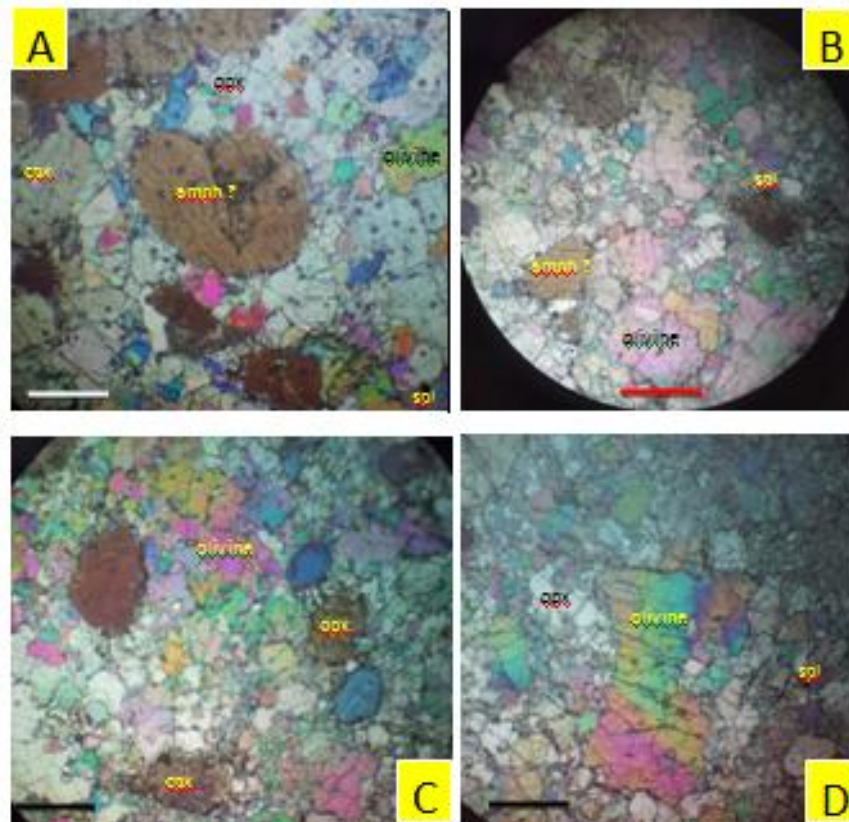


Fig. 2. A: Panoramic view of the north hillside of Djalsoka volcano, B: Sub-angular, C: Sub-rounded, and D: Rounded shape of studied peridotite xenoliths. Scale indicated by a coin

Table 1. Coordinates of the Lake Guinnadji and Ngao Djalsoka volcano peridotite xenoliths

Site	Sample	Coordinate
Lake Guinnadji	HD1	N07°09'35" E13°44'32"
Lake Guinnadji	HD2	N07°09'34" E13°44'34"
Lake Guinnadji	HD3	N07°09'33" E13°44'35"
Lake Guinnadji	HD5	N07°09'30" E13°44'33"
Djalsoka volcano	MO-12	N07°10'35" E13°45'06"
Djalsoka volcano	MO-03	N07°10'45" E13°45'23"
Djalsoka volcano	MO-10	N07°10'45" E13°45'29"





**Fig. 3. Photomicrographs of Lake Guinnadji and Ngao Djalsoka xenolith textures. A and B: Protogranular, C and D: Porphyroclastic textures. Scale bar represents 1 mm. amph = amphibole, cpx = clinopyroxene, opx = orthopyroxene, spl = spinel**

Olivine crystals (4 to 6 mm) are the most abundant component (74-86%, Table 2). The aggregates of small (< 1 mm) recrystallized olivine crystals show mosaic-shaped with straight-lined boundaries. A few (2-8%) clinopyroxene crystals (1 to 2 mm) occur in all samples especially in contact with the remnant orthopyroxene crystals. Orthopyroxene crystals (10-17%) are 2 to 4 mm-large. Large orthopyroxene crystals (4 mm) are mostly remnant and closely linked to olivine crystals. All samples are characterized by the occurrence of two kinds of olivine and enstatite crystals: large (6 mm) elongated and undulated grains (Fig. 3A

and D) and small (0.5-1 mm) generally polygonal strain ones (Fig. 3B and C) that might witness recrystallizations. Spinel (1-2%) is up to 1 mm in size. It always shows vermicular shape and frequently occurs between pyroxene crystals. Some spinels show dot shape feature Scarce amphibole (?) (2 to 3 mm in size, 0-1%) crystals occur in some samples (Fig. 3A). They are ovoid in shape and show small dots in their borders. Estimated volume percentages of mineral phases (Table 2), plot in the field of harzburgite in the Ol-Opx-Cpx ternary diagram (Fig. 4) of Le Maitre [20].

**Table 2. Modal compositions (in vol.%) of the studied peridotite xenoliths**

Locality	Sample	Olivine	Orthopyroxene	Clinopyroxene	Spinel	Amphibole
Guinnadji	HD1	85	10	3	1	1
Guinnadji	HD2	78	15	6	1	0
Guinnadji	HD3	86	11	2	1	0
Guinnadji	HD5	76	17	4	2	1
Djalsoka	MO-03	82	11	5	1	1
Djalsoka	MO-10	74	15	8	2	1
Djalsoka	MO-12	81	12	5	1	1

**Table 3. ICP-MS and ICP-AES analyses of whole rock major and trace elements and REE analyses of the Lake Guinnadji and Ngao Djalsoka volcano harzburgites and their CIPW normative compositions; note that LOI is negative as all Fe is measured as Fe<sub>2</sub>O<sub>3</sub>. The composition of Youkou lherzolite [7] is added for comparison**

Locality	Guinnadji	Guinnadji	Guinnadji	Guinnadji	Djalsoka	Djalsoka	Djalsoka	Youkou
Sample	HD1	HD2	HD3	HD5	MO-03	MO-10	MO-12	N-35
Rock	harzburgite	harzburgite	harzburgite	harzburgite	harzburgite	harzburgite	harzburgite	lherzolite
SiO <sub>2</sub> (wt %)	40.84	43.60	40.59	41.10	41.40	42.10	43.60	42.81
TiO <sub>2</sub>	0.07	0.14	0.06	0.15	0.15	0.21	0.18	0.04
Al <sub>2</sub> O <sub>3</sub>	0.62	1.54	0.66	0.71	0.67	1.23	1.45	2.05
Fe <sub>2</sub> O <sub>3</sub>	13.76	10.62	15.16	14.25	14.75	14.40	12.45	8.74
MnO	0.15	0.14	0.17	0.16	0.16	0.16	0.15	0.17
MgO	44.68	42.39	43.45	44.00	45.00	43.30	42.60	40.03
CaO	0.42	1.22	0.32	0.64	0.63	1.00	1.40	4.16
Na <sub>2</sub> O	0.08	0.21	0.10	0.16	0.18	0.26	0.23	0.18
K <sub>2</sub> O	0.05	0.10	0.08	0.09	0.08	0.13	0.09	0.02
P <sub>2</sub> O <sub>5</sub>	0.03	0.04	0.03	0.05	0.06	0.07	0.05	0.86
LOI	-1.10	-0.70	-1.00	-1.16	-1.21	-1.18	-1.00	0.23
sum	99.60	99.30	99.62	100.15	101.87	101.68	101.20	99.29
Mg#	86.57	88.77	85.02	85.92	85.79	85.65	87.14	90.03
CIPW norm								
Plagioclase	1.89	4.77	1.99	2.33	2.33	4.03	4.63	6.28
Orthoclase	0.30	0.59	0.47	0.53	0.47	0.77	0.53	0.12
Diopside	0.53	2.24	0.20	1.51	1.55	2.14	3.13	8.08
Hypersthene	12.09	21.21	13.25	11.35	9.40	11.94	18.54	16.32
Olivine	79.04	65.70	77.19	78.30	81.78	76.45	68.89	61.96
Ilmenite	0.13	0.27	0.11	0.28	0.28	0.40	0.34	0.08
Magnetite	6.64	5.12	7.32	6.89	7.12	6.96	6.00	4.20
Apatite	0.07	0.09	0.07	0.12	0.14	0.16	0.12	2.02
Be (ppm)	1	1	1					
Rb	0.8	1.8	1.6	2.1	2.5	4.3	2	
Sr	15.7	33.2	14.5	47.3	49.1	85.5	49.1	105
Cs	0.1	0.1	0.1	0.03	0.03	0.05	0.01	14.9
Ba	8	17	8	33.1	34.8	60.2	30.1	24
V	15	38	16	16	15	28	53	52

Locality	Guinnadji	Guinnadji	Guinnadji	Guinnadji	Djalsoka	Djalsoka	Djalsoka	Youkou
Sample	HD1	HD2	HD3	HD5	MO-03	MO-10	MO-12	N-35
Rock	harzburgite	harzburgite	harzburgite	harzburgite	harzburgite	harzburgite	harzburgite	lherzolite
Cr <sub>2</sub> O <sub>3</sub> (wt %)	0.057	0.313	0.028	0.042	0.032	0.071	0.177	0.2643
Co	146.7	119.2	168.9					114
Ni	2356	2309	2111					2408
Y	0.6	1.1	0.8	1.5	1.6	2.6	1.8	3
Zr	5.6	10.3	15.2	15	17	29	18	16
Hf	0.1	0.2	0.4	0.3	0.4	0.6	0.5	0.076
Nb	1.6	2.6	2.4	4.1	4.3	7.7	4.4	0.48
Ta	0.1	0.2	0.1	0.1	1	0.3	0.3	0.182
Th	0.1	0.2	0.3	0.41	0.46	0.74	0.4	0.27
U	0.1	0.1	0.1	0.15	0.28	0.22	0.12	0.101
La	1.5	2.2	2	3.3	3.9	6.2	3.6	2.46
Ce	2.1	4.4	3.6	6.7	7.6	12.2	7	4.85
Pr	0.18	0.51	0.34	0.73	0.85	1.46	0.83	0.45
Nd	1	2	1.3	3	3.2	5.4	3.2	1.51
Sm	0.07	0.32	0.13	0.62	0.61	1.23	0.53	0.193
Eu	0.05	0.12	0.06	0.17	0.15	0.27	0.22	0.083
Gd	0.2	0.26	0.15	0.35	0.54	0.93	0.42	0.29
Tb	0.03	0.05	0.02	0.06	0.05	0.12	0.06	
Dy	0.13	0.23	0.12	0.33	0.26	0.57	0.35	0.35
Ho	0.02	0.05	0.02	0.06	0.06	0.1	0.09	0.086
Er	0.07	0.15	0.07	0.12	0.15	0.22	0.21	0.24
Tm	0.01	0.01	0.01	0.02	0.02	0.03	0.03	
Yb	0.05	0.13	0.07	0.1	0.15	0.18	0.17	0.24
Lu	0.01	0.01	0.01	0.02	0.02	0.03	0.03	0.046
Ga	0.7	1.8	0.9	1.5	1.5	2.8	2.7	1
Sn	1	1	1	<1	<1	<1	<1	
Sc	7	9	7					14.9
W	0.5	0.5	0.6	<1	<1	<1	1	
Al <sub>2</sub> O <sub>3</sub> /MgO	0.01	0.04	0.02	0.02	0.01	0.03	0.03	0.05
Al <sub>2</sub> O <sub>3</sub> /TiO <sub>2</sub>	8.86	11.00	11.00	4.73	4.47	5.86	8.06	51.25
CaO/Al <sub>2</sub> O <sub>3</sub>	0.68	0.79	0.48	0.90	0.94	0.81	0.97	2.03
CaO/MgO	0.01	0.03	0.01	0.01	0.01	0.02	0.03	0.10

Locality	Guinnadji	Guinnadji	Guinnadji	Guinnadji	Djalsoka	Djalsoka	Djalsoka	Youkou
Sample	HD1	HD2	HD3	HD5	MO-03	MO-10	MO-12	N-35
Rock	harzburgite	harzburgite	harzburgite	harzburgite	harzburgite	harzburgite	harzburgite	lherzolite
Na <sub>2</sub> O/Al <sub>2</sub> O <sub>3</sub>	0.13	0.14	0.15	0.23	0.27	0.21	0.16	0.09
Na <sub>2</sub> O/TiO <sub>2</sub>	1.14	1.50	1.67	1.07	1.20	1.24	1.28	4.50
Ba/Rb	10.00	9.44	5.00	15.76	13.92	14.00	15.05	
Nb/Ta	16.00	13.00	24.00	41.00	4.30	25.67	14.67	2.64
Nb/Th	16.00	13.00	8.00	10.00	9.35	10.41	11.00	1.78
Sr/Nd	15.07	16.60	11.15	15.77	15.34	15.83	15.34	69.54
Y/Ho	30.00	22.00	40.00	25.00	26.67	26.00	20.00	34.88
Y/Nb	0.38	0.42	0.33	0.37	0.37	0.34	0.41	6.25
Zr/Hf	56.00	51.50	38.00	50.00	42.50	48.33	36.00	210.53
GdN/YbN	1.62	1.24	3.46	3.31	2.48	3.32	1.90	0.91
LaN/SmN	13.49	4.33	9.69	3.35	4.03	3.17	4.28	8.02
LaN/YbN	20.25	11.42	19.29	22.28	17.55	23.25	14.29	6.92
TbN/YbN	2.65	1.70	1.26	2.65	1.47	2.94	1.56	0.00

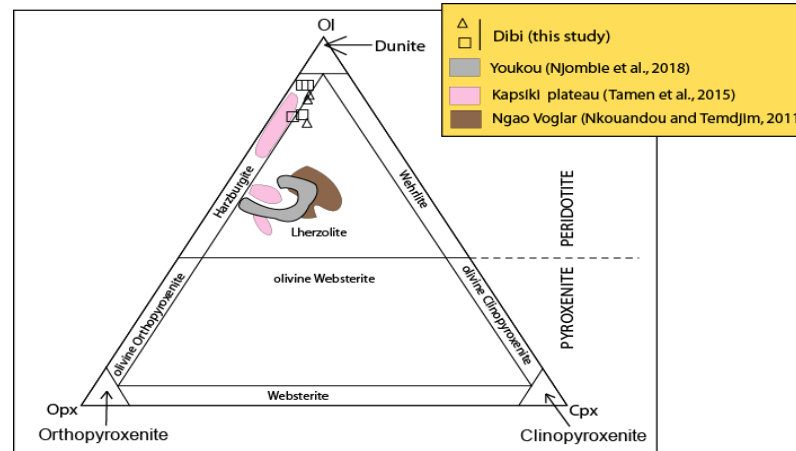


Fig. 4. Nomenclature of studied peridotite xenoliths according to the classification scheme of Le Maitre (2002). Dibi (this study): Lake Guinnadji (square) and Ngao Djalsoka volcano (triangle). Data from Youkou, Kapsiki plateau and Ngao Voglar are added for comparison



### 4.3 Geochemical Studies

Geochemical composition of xenoliths from the vicinity of Lake Guinnadji and Djalsoka volcano is listed in Table 3. Major elements contents show variable values. SiO<sub>2</sub> is between 40.59 and 43.60 wt.%. TiO<sub>2</sub> contents are relatively low (< 0.21 wt.%), samples HD1 and HD3 exhibit the lowest TiO<sub>2</sub> values (0.07-0.06 wt.%). Al<sub>2</sub>O<sub>3</sub> contents witness of two groups, low contents (0.62-0.71 wt.% for samples HD1, HD3, HD5 and MO-03) and relatively high contents (1.23-1.54 wt.% for samples HD2, MO-10 and MO-12). Note that CaO contents vary in the same way as Al<sub>2</sub>O<sub>3</sub>. The highest amounts of Al<sub>2</sub>O<sub>3</sub> and CaO correspond to the highest amounts of modal clinopyroxene (5-8 against 2-5 vol.% in the other group, see Table 2). These variations lead to CaO/Al<sub>2</sub>O<sub>3</sub> ratios between 0.68 and 0.97, with the mean value close to the Primitive upper mantle value of 0.80 [21]. Al<sub>2</sub>O<sub>3</sub>/TiO<sub>2</sub> ratio varies between 4.47 and 11.00.

Total Fe as Fe<sub>2</sub>O<sub>3</sub> contents are relatively constant (10.6-15.2 wt.%). MnO contents are low

and constant (0.14-0.17 wt.%). MgO contents are high with some variations, leading to Mg# ( $=100 \cdot (\text{MgO}/40.304) / ((\text{MgO}/40.304) + (\text{FeO}t/71.844))$ ) between 85.0 and 88.8.

Alkali contents Na<sub>2</sub>O (0.08-0.26 wt.%) and K<sub>2</sub>O (0.05-0.13 wt.%) are low for both Lake Guinnadji and Djalsoka volcano. Na<sub>2</sub>O/Al<sub>2</sub>O<sub>3</sub> ratio ranges between 0.13 and 0.27, compared to 0.11 value of subcontinental mantle (McDonough, 1990). P<sub>2</sub>O<sub>5</sub> contents are low (0.03-0.07 wt.%).

SiO<sub>2</sub>, Al<sub>2</sub>O<sub>3</sub>, CaO, Na<sub>2</sub>O and TiO<sub>2</sub> contents of studied xenoliths have been plotted against their MgO content (Fig. 5). All Harker diagrams show rather negative trends with increasing MgO values.

CIPW normative analyses (Table 3) confirm petrographical observations. Normative olivine (65.7-81.8 wt.%) constitutes the major mineral phase. Normative hypersthene (9.4-21.2 wt.%) is more abundant than normative diopside (0.2-3.1 wt.%), that is typical of harzburgites.

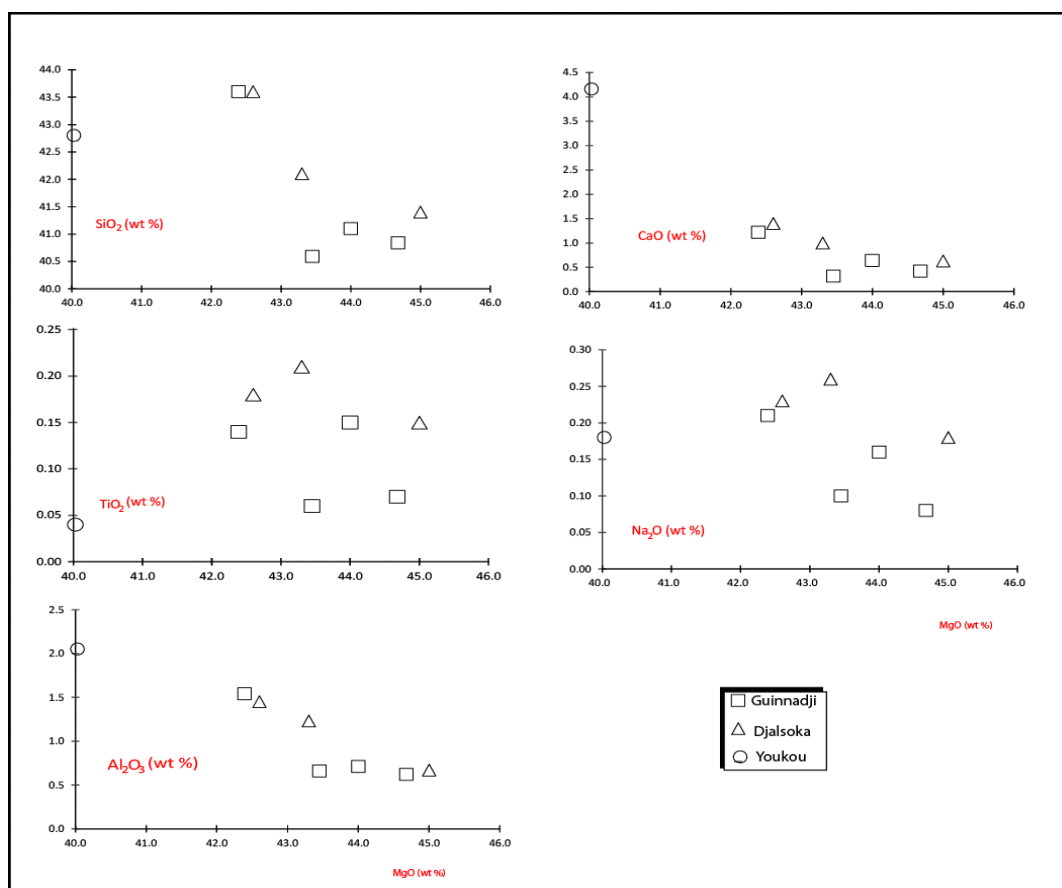


Fig. 5. Major oxide contents vs MgO content Harker diagrams of the Lake Guinnadji and Ngao Djalsoka volcano xenoliths

First transitional elements (Sc, V, Ni, Co and Cr) contents of analysed samples vary widely (see Table 3). Sc contents (7-9 ppm) are low, Ni (2111-2356 ppm),  $\text{Cr}_2\text{O}_3$  (0.03-0.31 wt.%) and Co (119-169 ppm) contents are high, while V varies between 15-and 53 ppm. Incompatible trace elements contents are low and show wide variation: Rb: 0.8-4.3 ppm, Sr: 14.5-85.5ppm, Ba: 8-60 ppm, Cs: 0.01-0.1 ppm and Th: 0.1-0.74 ppm. Zr: 5.6-29 ppm and Hf: 0.1-0.6 ppm, giving relatively constant Zr/Hf ratio of 36-56. Nb and Ta contents are also low and give contrasting Nb/Ta ratio (4.3-41) while Nb/Th ratio (8-16) is fairly high. Y (0.6-2.6 ppm) and Ho (0.02-0.1 ppm) gives Y/Ho ratio of 20-40. Sr/Nd ratio (11.1-15.8) is close to mantle peridotite [22].

Normalized REE ratios of studied xenoliths are shown in Fig. 6A. Samples display large variations in REE distribution patterns. Overall, the xenoliths are strongly enriched in LREE (LaN/SmN = 3.2-13.5). Moreover, LaN/YbN ratio ranges between 11.42 and 23.25. Normalized La is up to 10 times the mantle value, especially for samples of the MO group (Djalsoka volcano) which are characterized by relatively high REE values compared to samples of the HD group (Lake Guinnadji) (Table 3 and Fig. 6A).

In primitive mantle-normalized spider diagram (Fig. 6B), normalized trace elements display rather regular decrease in values from U to Lu. Samples of MO group are characterized by negative anomalies in K, Ti and also in P. Compared with the samples of MO group, HD group samples display negative anomalies in Ta and positive anomalies in Cs except HD5. All samples exhibit positive anomalies in Zr and most of them for U, except MO-10 and MO-12.

## 5. DISCUSSION

Geophysical studies carried out on the Adamawa plateau [2,23,24,3,25] have evidenced the reworking of Pan African faults which have crosscut the Adamawa basement and reach the lithospheric mantle, serving as pathways for the ascending magmas [1]. The studied xenoliths might have been sampled in such conditions, probably during transpressional movements of those faults or after upwelling. It has previously been shown, from Iherzolite xenoliths equilibria, that the Moho discontinuity is shallow, 20 km beneath the Dibi locality [18,26] due to the whole Adamawa uplift after the reworking of Pan African faults [1], leading to the compositional evolution of Adamawa subcontinental mantle [5].

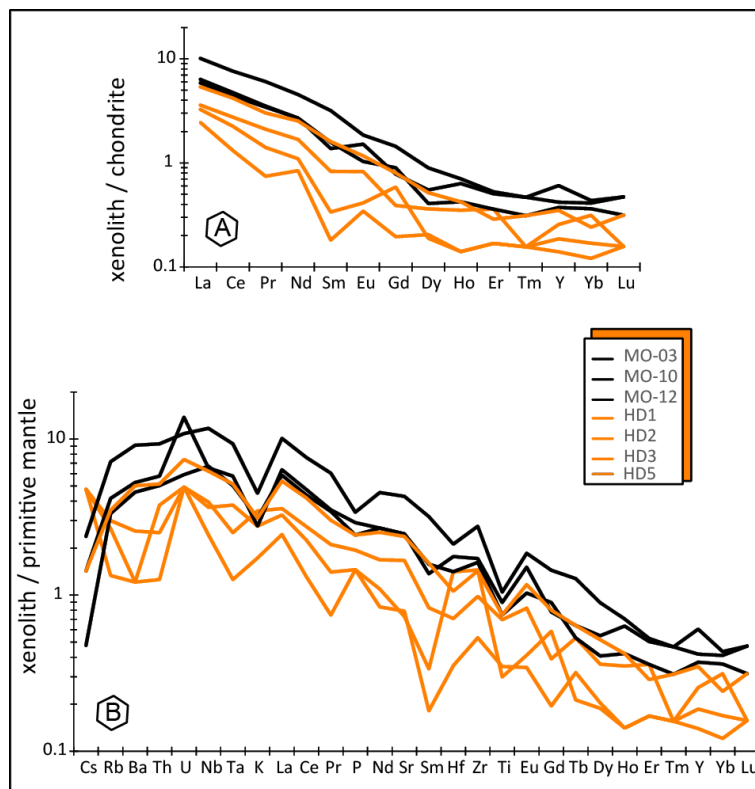


**Fig. 6. Chondrite-normalized REEs (a) and primitive mantle-normalized trace elements (b) abundances of the studied peridotite xenoliths according to McDonough and Sun [21]**

Petrographic and geochemical features of peridotite xenoliths sampled around the Lake Guinnadji and Ngao Djalsoka volcano witness of the complex nature of subcontinental mantle beneath the Dibi volcanic area. Field data show that peridotite xenoliths occur mainly in the pyroclastite projections exhibiting porous structure. Their sub-rounded or sub-angular shape may reflect the different sample depths within the mantle. Modal and normative analyses (Tables 2 and 3) point out far higher amount of orthopyroxene than that of clinopyroxene, which is typical of harzburgite type.

Geochemical data show some variation ranges of major and trace elements (Table 3, Fig. 5), which are certainly linked to the compositional diversity of mantle or processes. Geochemical compositions of studied harzburgite xenoliths characterize clearly that materials originated from a depleted mantle. MgO contents (42.4- 45.0 wt.% for Mg# (85.0-88.8) are close to typical harzburgite mantle (45-47 wt.% MgO for Mg# > 85, Maaløe and Aoki, [27]; McDonough, [28]). As a comparison, Youkou lherzolite presents a higher Mg# ratio of 90.0 for a lower MgO content of 40.0 wt.% (Table 3).

Studied xenoliths exhibit protogranular and porphyroclastic textures which are diagnostic for the mantle peridotites [29]. Remnants and recrystallized features of crystal phases may be interpreted as tectonic markers of their evolutionary setting.

Low contents of incompatible elements and their ratios (Zr/Hf, Nb/Ta, Y/Ho, Sc/Nd) are arguments in favor of mantle materials origin [21] of Lake Guinnadji and Ngao Djalsoka volcano peridotites instead of upper mantle fractional crystallization cumulates. The cumulate origin of studied xenoliths is excluded if one considers that all xenoliths exhibit an overall depletion in the HREE, resulting in higher LaN/YbN ratio (11.5-23.3) similar to those of fertile peridotite xenoliths worldwide [29].

K<sub>2</sub>O vs MgO diagram (Fig. 7) is used to discriminate xenoliths of cumulate origin from those of off-craton or cratonic origins (after Downes et al., [30]; see discussions in Lee et al., [31]; Downes, [32]). The studied xenoliths are clearly residual peridotites of off-craton origin. According to La vs Yb diagram (Fig. 8), almost all xenolith samples fall almost within the field of subcontinental harzburgite composition.

The studied xenoliths exhibit low values of CaO/MgO ratio (0.01-0.03), close to those of residual harzburgite peridotites (CaO/MgO < 0.02; Lenoir et al., [33]) and relatively high MgO contents (42.4-45.0 wt.%) compared to samples which have not experienced extensive loss of a basaltic component with ≤ 40.5-41.0 wt.% MgO [27,21]. REE data with strong LREE enrichment and LREE/HREE fractionation of the bulk rocks distinguish the Lake Guinnadji and Ngao Djalsoka peridotites as metasomatized harzburgites, as proposed by Downes [32] for the ultramafic xenoliths from Western and Central Europe.

Mg# vs CaO (wt.%) diagram (Fig. 9) and very high LaN/YbN ratio shows that the Lake Guinnadji and Ngao Djalsoka peridotites have experienced a rather high partial melting degree, between 20 and 30% (Fig. 9), and were modified by secondary enrichment process [21]. The contrasting geochemical signatures of the studied peridotites (Fig. 5) cannot be attributed to melt depletion or only partial melting processes. Rather, the observed enrichments of LREE and incompatible elements strongly reflect the effect of subsequent metasomatism of the Lake Guinnadji and Ngao Djalsoka volcano peridotites [34]. The occurrence of hydrous phase (amphibole?), suggested in the studied xenoliths, is known in upper mantle [35]. Spider diagrams (Fig. 6) show variable enrichment of incompatible elements especially positive anomalies in U and negative anomalies in Ta leading to variable degrees of cryptic metasomatism [34]. Subcontinental mantle under the Dibi locality might have evolved through two mantle processes: (1) varying degrees of depletion of a fertile mantle by extraction of basaltic melts, leaving a refractory residue, as shown by the systematic negative trends of CaO, SiO<sub>2</sub>, Al<sub>2</sub>O<sub>3</sub>, TiO<sub>2</sub> and Na<sub>2</sub>O and (2) modal metasomatism superimposed of the cryptic type. Silicate fluids induce the cryptic type metasomatism, according to relatively higher ratios of Na<sub>2</sub>O/Al<sub>2</sub>O<sub>3</sub> (0.13-0.27) than the 0.11 value of primitive mantle [28], relatively to carbonate type as CaO/Al<sub>2</sub>O<sub>3</sub> ratio of analysed samples is close to primitive mantle values (0.80). Moreover, high Zr/Hf (=36-56) and Nb/Ta (=4.3-225.7), which vary relatively to mantle values (Zr/Hf=36.30 and Nb/Ta= 17.5, Sun and McDonough, [36]), are interpreted as the result of pervasive silica melt-solid interaction with significant amounts of trapped melt. The MO-03 sample with low Nb/Ta (4.3) might have interacted with a limited amount of trapped melt [37].

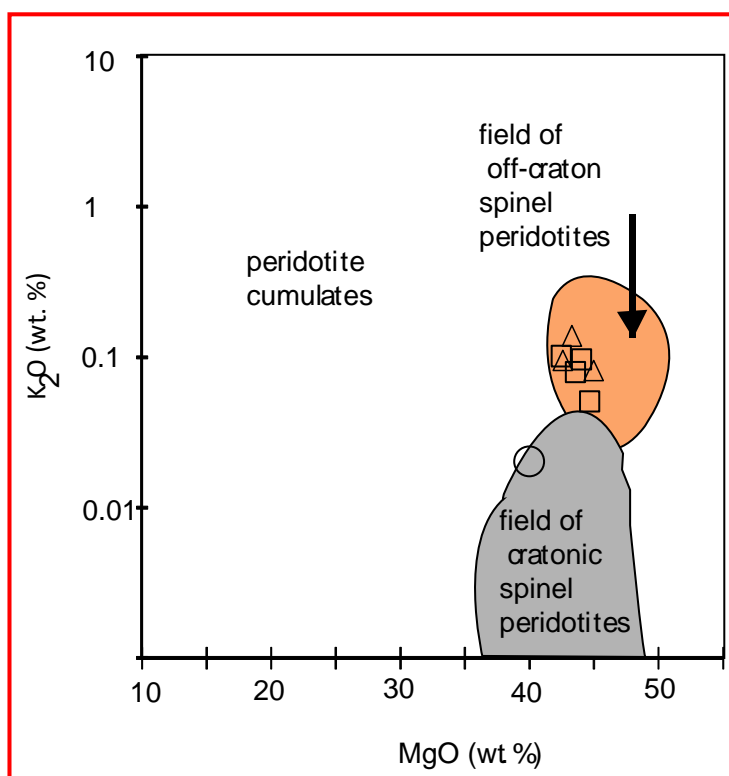


Fig. 7.  $K_2O$  vs  $MgO$  diagram for studied xenoliths. Lake Guinnadji (square), Ngao Djalsoka volcano (triangle), Youkou (circle). Fields of off-craton and cratonic mantle spinel peridotites from Downes et al. [30]. Compositions outside of these fields correspond to cumulates

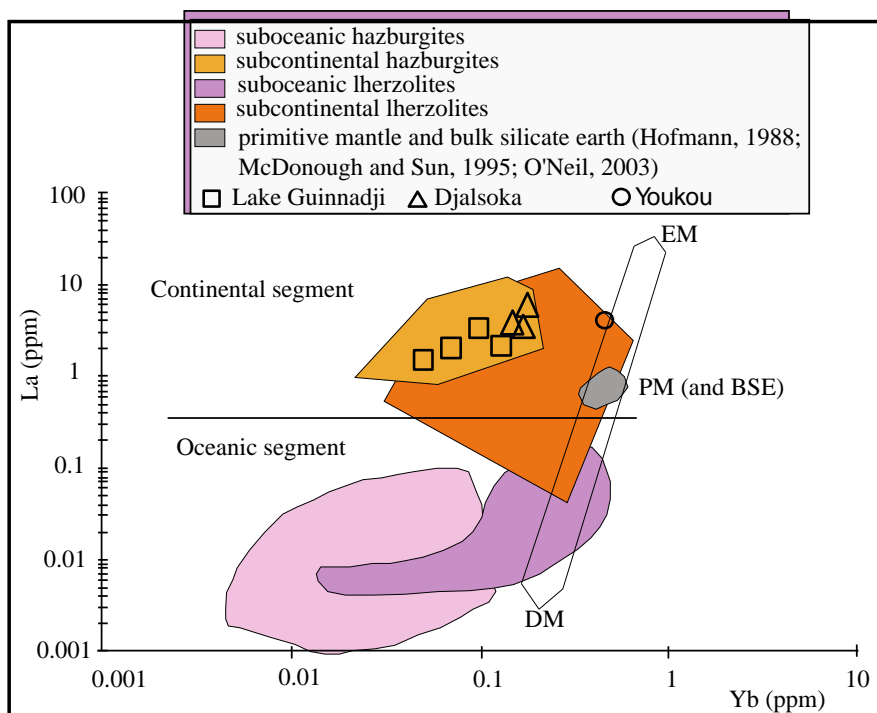
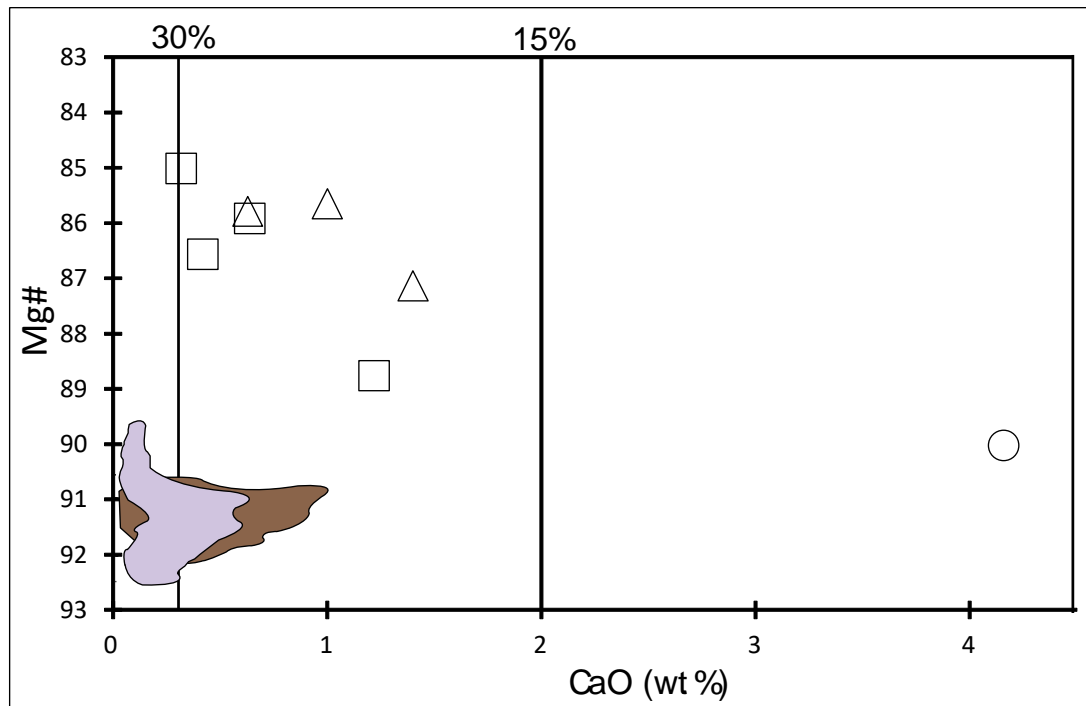


Fig. 8. Peridotite xenoliths from Ngao Djalsoka and Lake Guinnadji plotted in La vs Yb diagram after Balashov [38]. Youkou lherzolite [7] is plotted for comparison. BSE = Bulk Silicate Earth "pyrolite", DM-EM line = Depleted Mantle - Enriched Mantle



**Fig. 9. Mg# vs CaO (wt.%) diagram for Lake Guinnadji and Ngao Djalsoka peridotites. Same symbols as in Figure 8. Added for comparison: Youkou Iherzolite (circle, Njombie et al., [7]), Torishima and Conical Seamount: the dark gray shaded area corresponds to harzburgite, and the light grey shaded area to dunite [39]. Percentages of partial melting from a primitive source are indicated by the line at the top [40]**

## 6. CONCLUSION

Petrographic and geochemical preliminary data on the protogranular and porphyroclastic textured peridotite xenoliths from the Lake Guinnadji and Ngao Djalsoka volcano point their mantle origin. Rock-forming minerals are essentially olivine and orthopyroxene, and minor amount of clinopyroxene, spinel, plus amphibole (?). Studied xenoliths are harzburgite-type peridotites that have undergone high-degree partial melting, between 20 and 30%, and have been modified by secondary enrichment processes. The subcontinental mantle under the Dibi locality has evolved through varying degrees of depletion of a more fertile mantle by extraction of basaltic melts and modal metasomatism superimposed on the cryptic-type.

## ACKNOWLEDGEMENTS

Authors greatly thank the Acme Labs of Vancouver, Canada for ICP-MS and ICP-AES analyses. This paper is part of HA thesis. "Laboratory GEOPS" of the University Paris-Saclay, France is thanked for financial support of thin sections and ongoing microprobe analyses.

"B. Bonin and Reviewers are also thanked for their useful observations".

## COMPETING INTERESTS

Authors have declared that no competing interests exist.

## REFERENCES

1. Moreau C, Regnault JM, Déruelle B, Bobineau B. A new tectonic model for Cameroon line, central Africa. *Tectonophysics*. 1987;139:317-334.
2. Dorbath C, Dorbath L, Fairhead JD, Stuart GW. A teleseismic delay time study across the Central African Shear Zone in the Adamawa region of Cameroon, West Africa. *Geophysical Journal of the Royal Astronomical Society*. 1986;86:751-766.
3. Nnange JM, Ngako V, Fairhead JD, Ebinger CJ. Depths to density discontinuities beneath the Adamawa Plateau region, Central Africa, from spectral analyses of new and existing gravity data. *Journal of African Earth Sciences*. 2000;30(4):887-901.

4. Nkouandou OF, Ngounouno I, Déruelle B. Géochimie des laves basaltiques récentes des zones Nord et Est de Ngaoundéré (Plateau de l'Adamaoua, Cameroun, Afrique Centrale): pétrogenèse et nature de la source. *International Journal of Biological and Chemical Sciences*. 2010;4(4):984-1003.
5. Njankouo Ndassa ZN. Pétrologie et géochimie des péridotites mantelliques en enclaves dans les basaltes au nord de Ngaoundéré: nature du manteau subcontinental du plateau de l'Adamaoua (Plateau de l'Adamaoua, Cameroun, Afrique centrale). Thèse de l'Université de Ngaoundéré, Cameroun 232 pp +annexe; 2020.
6. Nkouandou OF, Bardintzeff JM, Fagny AM. Sub-continental lithospheric mantle structure beneath the Adamawa plateau inferred from the petrology of ultramafic xenoliths from Ngaoundéré (Adamawa plateau, Cameroon, Central Africa). *Journal of African Earth Sciences*. 2015;111:26-40.
7. Njombie MPW, Temdjim R, Foley SF. Petrology of spinel lherzolite xenoliths from Youkou volcano, Adamawa Massif, Cameroon Volcanic Line: Mineralogical and geochemical fingerprints of sub-rift mantle processes. *Contributions to Mineralogy and Petrology*. 2018;218:173-193.
8. Nkouandou OF, Temdjim R. Petrology of spinel lherzolite xenoliths and host basaltic lava from Ngao Voglar volcano, Adamawa Massif (Cameroon Volcanic Line, West Africa): equilibrium conditions and mantle characteristics. *Journal of Geosciences*. 2011;56:375-387.
9. Kampunzu AB, Popoff M. Distribution of the main Phanerozoic African rifts and associated magmatism: introductory notes. In: Kampunzu A.B. and Lubala R.T. (Eds.) *Magmatism in extensional structural settings. The Phanerozoic African plate*. Springer Verlag, Berlin. 1991;2-10.
10. Déruelle B, Ngounouno I, Demaiffe D. The 'Cameroon Hot Line' (CHL): A unique example of active alkaline intraplate structure in both oceanic and continental lithospheres. *Comptes Rendus Géoscience*. 2007;339(9):589-600.
11. Toteu SF, Michard A, Bertrand JM, Rocci G. U/Pb dating of Precambrian rocks from northern Cameroon, orogenic evolution and chronology of the Pan-African belt of Central Africa. *Precambrian Research*. 1987;37(1):71-87.
12. Toteu SF, Van Schmus WR, Penaye J, Michard A. New U-Pb and Sm-Nd data from north-central Cameroon and its bearing on the pre-Pan African history of central Africa. *Precambrian Research*. 2001;108(1-2):45-73.
13. Toteu SF. Geochemical characterization of the main petrographical and structural units of Northern Cameroon: Implications for Pan-African evolution. *Journal of African Earth Sciences*. 1990;10(4):615-624.
14. Ganwa AA, Frisch W, Siebel W, Ekodeck GE, Cosmas SK, Ngako V. Archean inheritances in the pyroxene-amphibole bearing gneiss of the Méiganga area (Central North Cameroon): Geochemical and  $^{207}\text{Pb}/^{206}\text{Pb}$  age imprints. *Comptes Rendus Géoscience*. 2008;340:211-222.
15. Temdjim R, Boivin P, Chazot G, Robin C, Rouleau E. L'hétérogénéité du manteau supérieur à l'aplomb du volcan de Nyos (Cameroun) révélée par les enclaves ultrabasiques. *Comptes Rendus Géoscience*. 2004a;336:1239-1244.
16. Gouhier J, Nougier J, Nougier D. Contribution à l'étude volcanologique du Cameroun ('Ligne du Cameroun', Adamaoua), *Annales de la Faculté des Sciences de l'Université de Yaoundé, Cameroun*. 1974;17:3-48.
17. Nkouandou OF, Ngounouno I, Déruelle B, Ohnenstetter D, Montigny R, Demaiffe D. Petrology of the Mio-Pliocene Volcanism to the North and East of Ngaoundéré (Adamawa-Cameroon). *Comptes Rendus Géoscience*. 2008;340:27-38.
18. Girod M, Dautria JM, Ball E, Soba D. Estimation de la profondeur du Moho, sous le massif volcanique de l'Adamaoua (Cameroun), à partir de l'étude d'enclaves de lherzolite. *Comptes Rendus de l'Académie des Sciences, Paris*. 1984;298(II,16):699-704.
19. Temdjim R, Njilah IK, Kamgang P, Nkoumbou C. Données nouvelles sur les laves felsiques de Ngaoundéré (Adamaoua, ligne du Cameroun): chronologie K-Ar et pétrologie. *African Journal of Science and Technology*. 2004b;5(2):113-123.
20. Le Maitre RW. (Ed.), *Igneous Rocks, A Classification and Glossary of Terms*. (Recommendations of the IUGS



- Subcommission on the Systematics of Igneous Rocks). Cambridge University Press, Cambridge. 2002;252.
21. McDonough WF, Sun SS. The Composition of the Earth, *Chemical Geology*. 1995;120:223-253.
  22. Jochum KP, McDonough WF, Palme H, Spettel B. Compositional constraints on the continental lithospheric mantle from trace elements in the spinel peridotite xenolith. *Nature*. 1989;340:548-550.
  23. Poudjom Djomani YH, Diament M, Albouy Y. Mechanical behavior of the lithosphere Beneath the Adamawa Up lift (Cameroon, West Africa) based on gravity data. *Journal of African Earth Sciences*. 1992;15:81-90.
  24. Poudjom Djomani YH, Nnange JM, Diament M, Ebinger CJ, Fairhead JD. Effective elastic thickness and crustal thickness variation in west central Africa inferred from gravity data. *Journal of Geophysical Research*. 1995;100:22047-22070.
  25. Nnange JM, Poudjom Djomani YH, Fairhead JD, Ebinger C. Determination of the isostatic compensation mechanism of the region of the Adamawa dome, West Central Africa using the admittance technique of gravity data. *African Journal of Science and Technology*. 2001;1(4):29-35.
  26. Dautria JM, Girod M. Les enclaves de lherzolite à spinelle et plagioclase du volcan de Dibi (Adamaoua, Cameroun): Des témoins d'un manteau supérieur anormal. *Bulletin de Minéralogie*. 1986; 109(3):275-286.
  27. Maaløe S, Aoki K. The major element composition of the upper mantle estimated from the composition of lherzolites, *Contributions to Mineralogy and Petrology*. 1977;63:161-173.
  28. McDonough WF. Constraints on the composition of the continental lithospheric mantle. *Earth and Planetary Science Letters*. 1990;101:1-18.
  29. Mercier JCC, Nicolas A. Textures and fabrics of upper-mantle peridotites as illustrated by xenoliths from basalts. *Journal of Petrology*. 1975;16(2):454-487.
  30. Downes H, Macdonald R, Upton BGJ, Cox KG, Bodinier JL, Mason PRD, James D, Hill PG, Hearn Jr C. Ultramafic xenoliths from the Bearpaw Mountains, Montana, USA: Evidence for multiple metasomatic events in the lithospheric mantle beneath the Wyoming Craton. *Journal of Petrology*. 2004;45(8):1631-1662.
  31. Lee CT, Rudnick RL, McDonough WF, Horn I. Petrologic and geochemical investigation of carbonates in peridotite xenoliths from northeastern Tanzania. *Contributions to Mineralogy and Petrology*. 2000;139:470-484.
  32. Downes H. Formation and modification of the shallow sub-continental lithospheric mantle: A review of geochemical evidence from ultramafic xenolith suites and tectonically emplaced ultramafic massifs of western and central Europe. *Journal of Petrology*. 2001;42(1):233-250.
  33. Lenoir X, Garrido CG, Bodinier JL, Dautria JM, Gervilla F. The recrystallization front of the Ronda peridotite: Evidence for melting and thermal erosion of subcontinental lithospheric mantle beneath the Alboran Basin. *Journal of Petrology*. 2001;42:141-158.
  34. Meshesha D, Shinjo R, Orihashi Y. Geochemical and Sr–Nd–Pb isotopic compositions of lithospheric mantle: Spinel lherzolites in alkaline basalts from the northwestern Ethiopian plateau. *Journal of Mineralogical and Petrological Sciences*. 2014;109:241-257.
  35. Dawson JB, Smith JV. Upper-mantle amphiboles: A review. *Mineralogical Magazine*. 1982;45:35-46.
  36. Sun SS, McDonough WF. Chemical and isotopic systematics in ocean basalt: implications for mantle composition and processes. In: Saunders, A. D. & Norry, M. J. (Eds.) *Magmatism in the Ocean Basins*. Geological Society, London, Special Publications. 1989;42:313-345.
  37. Niu Y. Bulk-rock major and trace element compositions of abyssal peridotites: Implications for mantle melting, melt extraction and post-melting processes beneath Mid-Ocean Ridges. *Journal of Petrology*. 2004;45(12):2423-2458.
  38. Balashov YA. Development of a heterogeneity in the lithosphere: Geochemical evidence. *Petrology*. 2009; 17(1):90-100.
  39. Ishii T, Robinson PT, Maekawa H, Fiske R. Petrological studies of peridotites from diapiric serpentinite seamounts in the Izu-Ogasawara-Mariana Forearc, Leg 125. *Proceeding of the Ocean Drilling Program, Scientific Results*. 1992;125:445-485.

40. Friedman E, Polat A, Thorkelson DJ, Frei R. Lithospheric mantle xenoliths sampled by melts from upwelling asthenosphere: The Quaternary Tasse alkaline basalts of southeastern British Columbia, Canada. Gondwana Research. 2016;33:209-230.

© 2021 Adama et al.; This is an Open Access article distributed under the terms of the Creative Commons Attribution License (<http://creativecommons.org/licenses/by/4.0>), which permits unrestricted use, distribution, and reproduction in any medium, provided the original work is properly cited.

*Peer-review history:*

*The peer review history for this paper can be accessed here:*

*<https://www.sdiarticle5.com/review-history/81483>*